Am J Transl Res 2022;14(7):5164-5177
www.ajtr.org /ISSN:1943-8141/AJTR0143818

Original Article

Promoting the formation of Pi-stacking interaction to improve CTL cells activation between modified peptide and HLA

Ying Zhu[1*], Chang-Xin Huang[2*], Le Zhang[3], Ze-Fang Wang[4], Dong-Li Zhao[3], Fei Ding[2], Si-Yu Zhang[2], Yong-Qiang Li[2], Ling-Zhi Chen[5]

[1]Department of Oncology, The First Affiliated Hospital of Zhejiang Chinese Medical University, Hangzhou 310000, Zhejiang, China; [2]Department of Oncology, The Affiliated Hospital of Hangzhou Normal University, Hangzhou 310000, Zhejiang, China; [3]Master Class, Zhejiang Chinese Medical University, The Fourth School of Clinical Medicine, Hangzhou 310000, Zhejiang, China; [4]Master Class, Hangzhou Normal University, The School of Medicine, Hangzhou 3100000, Zhejiang, China; [5]Department of Blood Transfusion, The First Hospital of Jiaxing, Affiliated Hospital of Jiaxing University, Jiaxing 314000, Zhejiang, China. [*]Equal contributors.

Received April 28, 2022; Accepted June 23, 2022; Epub July 15, 2022; Published July 30, 2022

Abstract: Objective: This study aims to investigate the use of single residue substitution to promote the formation of pi-stacking interactions between peptides and Human leukocyte antigen (HLA)-A*2402 molecules to improve the affinity of peptides and HLA molecules, as well as the level of cytotoxic T lymphocyte (CTL) cells activated by peptides-HLA (p-HLA) complex. Methods: Molecular docking and molecular dynamics simulation were used to simulate and analyze the interactions and binding free energies between HLA-A*2402-restricted antigen peptides and HLA molecules, before and after the single residue substitution. HLA-A*2402 restricted antigen peptides before and after the single residue replacement were loaded into dendritic cells (DCs) in vitro, and further Enzyme-Linked ImmunoSpot (ELispot) test was carried out to evaluate the effect of modified antigen peptides on the immune activation of CTL cells. Result: After replacing the antigen peptides with a single residue, some of them could promote the formation of pi-stacking interaction. The binding free energy between the modified antigen peptides and HLA-A*2402, as well as the level of immune activation of CTL cells were mostly higher than before, especially after the replacement of the 9th residue of the polypeptide, such as C9F and C9W. There was a significant negative correlation between the level of activated CTL cells by modified antigen peptides and the total interaction amount of hydrogen bonds and salt bridges. Conclusion: Promoting the formation of pi-stacking interaction between antigen peptides and HLA-A*2402 molecules could increase the total binding free energy of p-HLA complex and the level of CTL cells activation. In addition, the amount of hydrogen bonds and salt bridges between peptides and HLA could reduce the level of immune activation. All the characteristics above can improve the immunogenicities of the weak antigens.

Keywords: Residue substitution, pi-stacking (π-stacking), T cell activation, molecular dynamics simulation

Introduction

Given the low rate of persistent tumor regression observed with immune checkpoint inhibitors (ICIs) in patients with advanced malignant tumors, combining that with other T cell immunotherapy, such as personalized cancer vaccines and adoptive transfusion of T cell receptor (TCR) engineered T cells, may improve the patients' prognosis [1]. At present, the characteristic parameters of the existing prediction tools are limited, and the HLA-restricted neoantigens with high HLA affinity and stability have not been accurately screened. One of the most frequently studied aspects of T cell tumor immunity is the intensity of the interaction between TCRs and their ligand peptide/MHC complex (pMHC). TCR/pMHC is the only receptor-ligand pair that determines T cell functional responses and antigen specificity. The firmness of TCR/pMHC interaction and the environment are the key to how T cells respond. Although the T cells interacting with tumor-associated antigens have a low affinity, the corresponding TCR

library is significant [2]. Specific interactions mediate adaptive immune recognition between heterodimer TCR and pMHC ligand. The accurate prediction of TCR: pMHC interaction will have far-reaching clinical significance [3]. The main challenge of neo-antigen immunotherapy was predicting the affinity and stability of p-HLA complex, as well as the level of activated CTL cells. It was primarily determined by a competitive binding test between many peptides and HLA learned by an artificial neural network. Although the prediction results were sensitive, they failed to fully clarify the characteristic parameters of the high immunogenicity of new tumor antigens. On the basis of our previous research progress [4], this study aimed to further discuss the method of replacing a single residue on the antigen peptides to promote the formation of pi-stacking interactions between peptides and HLA-A*2402 to improve the affinity of modified antigen peptides and HLA molecules, as well as the level of pHLA complex activating CTL cells. The parameters related to improving peptide-HLA affinity and CTL level activated by pHLA complex were further summarized. This study is committed to screen HLA-I-restricted neoantigen peptides with high HLA affinity, and may help improve the immunogenicity of neoantigens.

Materials and methods

Antigen peptides and unmethylated CpG synthesis

The antigen peptides were synthesized *in vitro* by the Chinese Peptide Company (Hangzhou, China). Unmethylated CpG was synthesized in vitro by Sangon Biotech Co., Ltd. (Shanghai, China). The sequence of unmethylated CpG (5'-3') was TCGTCGTTTTGTCGTTTTGTCGTTGGGG.

Antigen peptide sequences before/after residue replacement

HLA-A*2402-restricted antigen peptides are the epitopes of Human Papillomavirus viral (HPV) genome's conserved regions E6 and E7. Nine peptide sequences were found in literature [5]. The sequences of the two polypeptides were CYSLYGTTL and HYNIVTFCC, respectively. According to previous study [4], the pi-stacking interaction between peptides and HLA-A*2402 molecule was mainly caused by Tyrosine (Tyr, Y, the residues were located at the Position 2 (P2), P4, P5, and P7, respectively), Hlstidine (His, H, the residues were located at P1 and P3, respectively), Tryptophane (Trp, W, the residues were located at P2 and P9, respectively) and Phenylalanine (Phe, F, the residue located at P9) on the antigen peptides. However, P6 and P9, on the peptides, did not form pi-stacking with HLA-A*2402. P2, P4, P5 and P7 of the above two peptides were replaced by the method of single residue substitution of Y, P1 and P3 by H, P2 and P9 by W, and P9 by F. The sequences of 14 antigen peptides after residue substitution were as follows: CYSYYGTTL, CYSLYGYTL, HYSLYGTTL, CYHLYGTTL, CYSLYGTTF, CWSLYGTTL, CYSLYGTTW, HYNYVTFCC, HYNIYTFCC, HYNIVTYCC, HYHIVTFCC, HYNIVTFCF, HWNIVTFCC and HYNIVTFCW.

Molecular docking

The polypeptide structures were produced by rosetta (https://www.rosettacommons.org/), and the structures were checked by Python molecule (PyMOL, https://pymol.org/2/) and then converted to The Python Debugger (PDB) format. These were then Loaded into AutoDockTools-1.5.6 (https://autodock.scripps.edu/), after adding atomic charge, and assigning atomic type, all flexible bonds were rotated and saved as pdbqt format, as docking ligand, respectively. The crystal structure of HLA-A*2402 (PDB ID: 7JYV) was downloaded from Research Collaboration for Structural Bioinformatics (RCSB database, https://www.rcsb.org/structure/). Pymol was used to delete its crystal water and other small molecules, add hydrogen atoms, and convert to pdb format. Loading into AutoDock, adding atomic charge and assigning atomic type, it was then saved as pdbqt format, as docking acceptor. The exhaustiveness parameter was set to 32 by Autodock, and the other parameters were default. The docking box was set to wrap HLA bonding grooves completely, and the conformation with the highest score was chosen as the docking conformation for molecular dynamics simulation. Maestro 11.5 (https://www.schrodinger.com/training/maestro11/home) was used to analyze the interface between peptides and HLA, and the software automatically recognized peptide as a ligand, and HLA as a receptor, respectively. It selected the protein interaction analysis from the task menu to analyze and export the file in csv format.

Molecular dynamics simulation

Amber18 (https://ambermd.org/) simulated HLA complex obtained through molecular docking. To neutralize the charge, the peptides and HLA molecule were loaded into the tleap with the force field parameters of ff14sb, an automatically added hydrogen atom, and sodium ions were added. The dominant water model TIP3P was selected, and the periodic boundary condition was set. The nearest distance between the boundary of water box and the molecule was no less than 1 nm. First, the heavy atoms of proteins and peptides were constrained to minimize the energy of water molecules in 10000 steps (including 5000-step of steepest descent and 5000-step of conjugate gradient). Then, the constraint was released, and 10000-step energy minimization of the whole system was carried out (including 5000-step of steepest descent and 5000-step of conjugate gradient). Following energy minimization, the system was slowly heated to 300K in 50ps. After the heating was completed, the system balance was performed at 50ps using Normal Pressure and Temperature (NPT) ensemble. Finally, a 20 ns molecular dynamics simulation was performed using NPT ensemble with a step of 2fs. The trajectory data were saved every 10ps, and the correlation analysis was performed using CPPTRAJ. The binding free energy of ligand and protein was calculated by Molecular Mechanics/Poisson-Boltzmann Surface Area (MM/PBSA).py, with HLA as the receptor and polypeptide as the ligand.

Differentiation of dendritic cells (DCs)

The anticoagulant tubes (Becton, Dickinson and Company, U.S., Cat. No: 367525) were filled with 10 mL of peripheral blood from healthy volunteers who were homozygote for HLA-A*2402 allele gene. Ficoll density gradient centrifugation (Tianjin Haoyang, China, Cat. No: LTS1077) was used to isolate peripheral blood mononuclear cells (PBMCs). The hospital ethics committee examined and approved this study (Approval No.: 2022-K-009-01. See the supplementary materials for details), and the volunteers signed the informed consent forms. PBMCs were resuscitated with Roswell Park Memorial Institute (RPMI)-1640 cell culture medium (Meilunbio, China, Cat. No: MB4374) containing 10% Fetal bovine serum (FBS) (Gemini, U.S., Cat. No: 900-108), then cultured in 24-well plates (Corning, U.S., Cat. No: 3527) with 2×10^6 cells per well. After 10 hours (h), non-adherent cells were discarded after putting into the cell incubator (Thermo Fisher, U.S., Cat. No: 3111) at 37°C and with 5% CO_2. The cell culture plate was washed with the preheated medium two times. Then, 100 ng/mL rh Granulocyte-Macrophage Colony Stimulating Factor (GM-CSF, Sino Biological, China, Cat. No: 10015-HNAH), 100 ng/mL rh Interleukin-4 (IL-4, Sino Biological, China, Cat. No: 11846-HNAE), 50 ng/mL gentamicin (Gibco, U.S., Cat. No: R01510), 50 μM/L β-mercaptoethanol (aladdin, China, Cat. No: 60-24-2), and 10% FBS were added into RPMI-1640 culture medium. The cells were cultured overnight, and the unattached suspension cells were discarded and re-suspended for 1 day. The medium was changed by half the next day. When the cells were differentiated into the semi-suspended state, they were the immature DCs (imDCs).

DC vaccines preparation

Typically, 100 μg antigen peptide, 100 μg CpG, and 50 ng/mL IFN-γ (Sino Biological, China, Cat. No: 11725-HNAS) were added to 1×10^4 cells per well to stimulate the cells. After 24 to 48 h, imDCs were loaded with antigens and then differentiated into mature DCs (mDCs), and the suspended mDCs were enriched as DC vaccines.

PBMCs stimulated by DC vaccines

DC vaccines with 1×10^6 cells per well were added to a 24-well plate. PBMCs of the same healthy volunteer with HLA-A*2402 allele homozygote were extracted and then added to DC vaccines with 5×10^6 cells per well. They were continued to cultivate in RPMI-1640 medium containing 10% FBS, 60 μg/L rhIL-2 (Sino Biological, China, Cat. No: 11848-HNAH1-E), 50 μg/mL gentamicin, and 50 μM/L β-mercaptoethanol. Every 5-7 days, DC vaccines were repeatedly stimulated with the same PBMCs, for two cycles. All cells were collected and gathered for ELispot test.

CTL activation detection

Each antigen peptide synthesized *in vitro* was set to three repetitive pores, and interferon

(IFN)-γ stimulation alone was used as control. By the Human IFN-γ precoated Enzyme-Linked ImmunoSpot (ELispot) kit (Dakewe Biotech Co., China, Cat. No: 1110002), all holes of ELispot plate were filled with 200 μL RPMI-1640 culture medium and incubated at room temperature for 20 minutes (min); all above cells were collected and centrifuged at 1500 rpm for 5 min. The cells were resuspended and washed once with RPMI-1640 culture medium, then, the final volume of cell suspension to 200 mL was adjusted, and RPMI-1640 culture medium was sucked out through the plate's holes. Typically, 200 μL mixed cells were added to each well. For 24 h, the cell culture plate was placed in the cell incubator of 5% CO_2 at 37°C. Each hole was washed with diluted wash buffer for five times. After the last wash, it was patted to dry on the absorbent paper. Following that, 100 μL diluted detection antibody was added to each hole and incubated overnight for 4°C. Each hole was washed with diluted wash buffer for five times. After the last wash, it was left to dry on the absorbent paper. Then, 100 μL diluted streptavidin-AP was added to each hole and incubated at room temperature for 2 h. Next, 300 μL phosphate-buffered saline (PBS) (Genom, China, Cat. No: GNM20012) was added to each hole and washed twice. Each hole was washed five times and then patted to dry on the absorbent paper. Following that, 100 μL 5-bromo-4-chloro-3-indolyl phosphate/Nitroblue tetrazolium chloride (BCIP/NBT) chromogen was added to each hole and incubated in dark at room temperature for 1 h. The chromogenic solution was discarded, rinsed with deionized water, and dried for 30 min at 37°C. The ELispot reader (Cellular Technology Limited, U.S., Cat. No: S6 Core Versa Micro UV) was applied to count the round spots with a dark center and blurred edges.

Statistical analysis

All data were processed by SPSS statistical software (SPSS 22.0, IBM, https://www.ibm.com/cn-zh/analytics/spss-statistics-software). If the index passed the normality and variance homogeneity tests, the analysis of variance was used; otherwise, the non-parametric test was used. The Pearson correlation coefficient was used to measures the strength of the correlation. $P < 0.05$ meant that the difference was statistically significant.

Results

The change of binding free energy of substituted single residue to HLA

As demonstrated in **Table 1**, P1 to P9 represented the binding free energy values (DELTA TOTAL) of single residues at positions 1 to 9 of antigen peptides to HLA, respectively. Before and after the replacement, the binding energy difference was the energy of a single residue before replacement minus that of a single residue after replacement. The positive values (difference > 2 KJ/mol) indicated that the interaction of residue after substitution to HLA was more substantial than before, and the opposite results were indicated as negative values (the difference < -2 KJ/mol). **Table 1** displays that the binding free energy of P2 was higher than that of other positions to HLA-A*2402, regardless of whether the residue was replaced. The differences in residue substitution of CYSLYGTTL were T7Y, C1H and L9F, and the ones of HYNIVTFCC were N3H, C9F, Y2W and C9W. The positive differences indicated that the interaction after substitution was stronger than before. The difference in HYNIVTFCC residue substitution was F7Y, and it was negative, indicating that the interaction after substitution was weaker than before.

Changes of binding free energy between modified peptide and HLA

Table 2 displays the binding free energy, various energy components, and the difference between the modified peptide and HLA-A*2402 molecule before and after substitution. Among them, the differences in total binding free energy (DELTA TOTAL), van der Waals force (VDWAALS), electrostatic interaction (EEL), polar solvation energy (EGB), non-polar solvation energy (ESURF), gas-free energy (DELTA G gas) and solvation free energy (DELTA G solv) were the energy value before antigen modification - the energy value after antigen modification. The positive value indicated that the modified peptide was easier to bind with HLA. In contrast, the negative value meant that the modified peptide was more difficult to bind with HLA. The peptides with a significant difference in DELTA TOTAL were CYSYYGTTL, HYNIVTFCF, HWNIVTFCC and CYSLYGTTF. The peptides with a significant difference in VDWAALS were HYNIVTFCW, HYNIVTFCF and CYSLYGTTW. The pep-

Table 1. The changes of binding free energy of substituted single residue of antigens to HLA

No.	Before Residue Replacement-Position-After Residue Replacement	Peptide Sequences	The DELTA TOTAL of Substituted Single Residue of antigens to HLA (KJ/mol)									The Differences (KJ/mol)
			P1	P2	P3	P4	P5	P6	P7	P8	P9	
1	original	CYSLYGTTL	5.9309	-8.7640	-1.6174	-2.1732	-2.5158	0.1959	-0.4175	-3.6951	-5.4867	0.0000
2	L4Y	CYSYYGTTL	-0.2632	-8.8577	0.3157	-3.3426	-2.8036	-0.0163	0.0578	-4.6806	-5.7033	1.1694
3	T7Y	CYSLYGYTL	4.8652	-8.9756	-1.0187	-2.5826	-2.4468	-0.0433	-2.7629	-4.7319	-4.3043	2.3454
4	C1H	HYSLYGTTL	0.4254	-8.1868	-0.7750	-2.0547	-2.1632	0.2885	0.1072	-3.6883	-6.2592	5.5055
5	S3H	CYHLYGTTL	1.0184	-6.8079	-3.3624	-3.6988	-2.8751	-0.2498	0.1688	-3.2530	-6.0484	1.7450
6	L9F	CYSLYGTTF	1.0007	-8.9150	-0.7760	-2.9866	-2.5017	-0.2866	0.8682	-3.2877	-7.5637	2.0770
7	Y2W	CWSLYGTTL	3.2354	-8.3368	-1.6378	-1.8361	-3.2196	0.3185	-0.4937	-4.8172	-4.6861	-0.4272
8	L9W	CYSLYGTTW	1.6125	-7.7263	-1.1584	-3.1694	-3.2438	-0.4225	-1.1325	-3.0775	-6.2060	0.7193
9	original	HYNIVTFCC	-0.7859	-9.8423	-3.0672	-2.2803	-2.1042	-0.9871	-5.6656	-2.7745	-2.2985	0.0000
10	I4Y	HYNYVTFCC	-0.3811	-8.5407	-3.7383	-1.2200	-2.6761	-5.2090	-1.6483	-3.7231	-1.0485	-1.0604
11	V5Y	HYNIYTFCC	-0.1770	-10.3851	-3.4174	-2.8924	-1.9947	-0.9672	-3.7400	-3.7613	-2.6363	-0.1095
12	F7Y	HYNIVTYCC	-1.7153	-9.0351	-5.3494	-3.6606	-3.8570	-1.0932	-3.0295	-2.6064	-1.4157	-2.6361
13	N3H	HYHIVTFCC	1.1653	-8.7795	-6.4182	-2.7704	-3.5859	-1.2359	-3.0658	-3.6939	-2.3773	3.3510
14	C9F	HYNIVTFCF	-2.1514	-8.3732	-5.2364	-2.9960	-1.6362	-1.3473	-4.8609	-3.2181	-7.2989	5.0004
15	Y2W	HWNIVTFCC	-1.3761	-12.5799	-3.1783	-2.9493	-3.3492	-2.6466	-4.3264	-2.6591	-1.6825	2.7375
16	C9W	HYNIVTFCW	-2.5685	-9.0940	-2.8079	-3.0197	-2.1403	-1.0694	-3.8921	-3.1293	-5.6985	3.4000

Table 2. The changes of various components of energy between modified peptide and HLA

No.	Before Residue Replacement-Position-After Residue Replacement	Peptide Sequences	DELTA TOTAL (KJ/mol)	Differences of DELTA TOTAL (KJ/mol)	VDWAALS (KJ/mol)	Differences of VDWAALS (KJ/mol)	EEL (KJ/mol)	Differences of EEL (KJ/mol)	EGB (KJ/mol)	Differences of EGB (KJ/mol)	ESURF (KJ/mol)	Differences of ESURF (KJ/mol)	DELTA G gas (KJ/mol)	Differences of DELTA G gas (KJ/mol)	DELTA G solv (KJ/mol)	Differences of DELTA G solv (KJ/mol)
1	original	CYSLYGTTL	-65.9026	0	-86.4501	0	-326.6286	0	360.8166	0	-13.6405	0	-413.0787	0	347.1761	0
2	L4Y	CYSYYGTTL	-81.7822	15.8796	-96.4481	9.998	-353.852	27.2234	383.1798	-22.3632	-14.6619	1.0214	-450.3001	37.2214	368.5179	-21.3418
3	T7Y	CYSLYGYTL	-68.655	2.7524	-88.155	1.7049	-312.9645	-13.6641	345.9344	14.8822	-13.47	-0.1705	-401.1195	-11.9592	332.4645	14.7116
4	C1H	HYSLYGTTL	-68.1285	2.2259	-88.9018	2.4517	-333.2325	6.6039	367.6725	-6.8559	-13.6667	0.0262	-422.1343	9.0556	354.0058	-6.8297
5	S3H	CYHLYGTTL	-73.2687	7.3661	-90.5112	4.0611	-362.839	36.2104	394.2684	-33.4518	-14.1869	0.5464	-453.3502	40.2715	380.0815	-32.9054
6	L9F	CYSLYGTTF	-77.4269	11.5243	-92.1992	5.7491	-356.8651	30.2365	385.6163	-24.7997	-13.979	0.3385	-449.0642	35.9855	371.6373	-24.4612
7	Y2W	CWSLYGTTL	-61.1912	-4.7114	-80.917	-5.5331	-355.2427	28.6141	387.8594	-27.0428	-12.8909	-0.7496	-436.1597	23.081	374.9685	-27.7924
8	L9W	CYSLYGTTW	-68.5951	2.6925	-97.3238	10.8737	-344.6139	17.9853	387.7408	-26.9242	-14.3982	0.7577	-441.9377	28.859	373.3426	-26.1665
9	original	HYNIVTFCC	-84.9508	0	-93.8348	0	-350.3979	0	373.4433	0	-14.1614	0	-444.2327	0	359.2819	0
10	I4Y	HYNYVTFCC	-79.1179	-5.8329	-90.5582	-3.2766	-333.1227	-17.2752	358.4565	14.9868	-13.8935	-0.2679	-423.6809	-20.5518	344.563	14.7189
11	V5Y	HYNIYTFCC	-87.9024	2.9516	-96.9026	3.0678	-338.4068	-11.9911	362.0749	11.3684	-14.6679	0.5065	-435.3094	-8.9233	347.4071	11.8748
12	F7Y	HYNIVTYCC	-93.2683	8.3175	-96.2246	2.3898	-351.7215	1.3236	369.5807	3.8626	-14.9029	0.7415	-447.9461	3.7134	354.6778	4.6041
13	N3H	HYHIVTFCC	-84.4527	-0.4981	-94.8744	1.0396	-352.5559	2.158	377.1902	-3.7469	-14.2126	0.0512	-447.4303	3.1976	362.9776	-3.6957
14	C9F	HYNIVTFCF	-100.4423	15.4915	-105.905	12.0702	-350.2605	-0.1374	371.0272	2.4161	-15.304	1.1426	-456.1655	11.9328	355.7232	3.5587
15	Y2W	HWNIVTFCC	-96.6829	11.7321	-102.5453	8.7105	-353.6085	3.2106	374.6287	-1.1854	-15.1579	0.9965	-456.1538	11.9211	359.4708	-0.1889
16	C9W	HYNIVTFCW	-93.5916	8.6408	-110.8551	17.0203	-332.4705	-17.9274	365.2608	8.1825	-15.5268	1.3654	-443.3256	-0.9071	349.734	9.5479

tides with a significant difference in EEL included CYHLYGTTL, CYSLYGTTF, CWSLYGTTL, CYSYYGTTL and CYSLYGTTW. The peptides with a significant difference in EGB included HYNYVTFCC, CYSLYGYTL and HYNIYTFCC. There was little difference in ESURF after residue replacement of antigens. The peptides with a significant difference in DELTA G gas comprised CYHLYGTTL, CYSYYGTTL, CYSLYGTTF, CYSLYGTTW, CWSLYGTTL, HYNIVTFCF and HWNIVTFCC. The peptides with a significant difference in DELTA G solv consisted of HYNYVTFCC, CYSLYGYTL and HYNIYTFCC.

Changes in docking parameters between modified peptide and HLA

As revealed in **Table 3**, most amino residues on the antigens that interacted with HLA were altered after modification. Except for CYSYYGTTL, CYHLYGTTL, HYNIYTFCC and HYHIVTFCC, the reformed peptide residues interacted with more HLA amino residues. Comparing the properties of differential residues on the modified peptides that interacted with HLA molecules, it was found that peptides before residue substitution mainly interacted with aromatic and aliphatic amino residues, such as Y, W, V, I and L on HLA. The reformed peptides containing substituted residues interacted not only with HLA mentioned above residues but also with amino residues containing hydroxyl, amide and sulfur.

As displayed in **Table 4**, The modified peptides formed pi-stacking with HLA were as follows: CYSLYGYTL, CYSLYGTTF, CYSLYGTTW, HYNIVTFCF, HWNIVTFCC and HYNIVTFCW.

Table 5 displays the changes in the ratio of surface complementarity (Surface Complementarity) and the decrease of solvent accessible area (Buried SASA) between the substituted residue of the antigen and HLA After residue substitution. The Surface Complementarity of some peptides to HLA were increased: CYSYYGTTL, HYNYVTFCC, HYNIVTFCF and HYNIVTFCW. The Buried SASA of some peptides to HLA was increased: HYNIVTFCF, CYSLYGYTL, HYNIVTFCW and HYNYVTFCC.

Changes in the number of CTL cells activated by modified peptides DC vaccines

The polypeptides before and after modification were respectively loaded on DCs of homozygous HLA-A*2402 alleles to prepare polypeptide vaccines and further activate CTL cells of the same donor for Elispot test. As depicted in **Figure 1** and **Table 6**, except for CYSLYGTTF, the spot values of other modified peptides were higher than those before replacement, especially CYSLYGTTW, HYNIVTFCW, HYNIVTYCC and HWNIVTFCC, and the differences were statistically significant.

Correlation analysis between CTL cell activation number and molecular aimulation parameters of peptides before and after modification

The changes in molecular simulation parameters of peptides before and after modification with HLA are depicted in **Table 7**, including the total number of HB, salt bridges, pi-stacking, vdW Clash, and the average values of Surface Complementarity and Buried SASA between modified antigens and HLA. As demonstrated in **Table 8**, there was a significant negative correlation between the spots number of CTL cells activation and the total number of HB and salt bridges.

Discussion

The existing peptide-MHC interaction predictors were primarily trained using binding affinity data, which included information about the processing steps of peptides in the presentation pathway and the length distribution of natural delivery peptides. NetMHCpan-4.0 was an affinity prediction model based on binding affinity and elution ligand data [6]. MHCflurry 2.0 [7] was a new model integrating MHC class I binding and antigen processing. The performance of integrated model was better than that of two separate components, NetMHCpan 4.0 and MixMHCpred 2.0.2. TruNeo [8] was used to identify and rank neoantigens from point mutation, insertion and deletion of genes, and fusion genes, considering every biological step involved in HLA molecules, tumor heterogeneity HLA-LOH and other factors. It was predicted that neoantigens at the top of the list were likely to have immunogenicity. TruNeo was thought to outperform MHCfurry in terms of predictive performance. ForestMHC prediction model [9] was based on a random forest classifier and performed better in the test set than NetMHC and NetMHCpan. It was related to the known chemical binding affinity and was better than the depth neural network method and convolution neural network method based on the same data training. For specific HLA allo-

Table 3. The changes of amino residues interacting with modified peptides on HLA

No.	Before Residue Replacement-Position-After Residue Replacement	Peptide Sequences	Closest amino residue on HLA before replacement	Closest amino residue on HLA after replacement
1	L4Y	CYSYYGTTL	A: 69: Ala A: 70: Hie	A: 69: Ala A: 70: Hie
2	T7Y	CYSLYGYTL	A: 147: Trp A: 73: Thr	A: 77: Asn (Amido, polarity without charge) A: 150: Ala (Aliphatic, non-polar) A: 147: Trp A: 73: Thr
3	C1H	HYSLYGTTL	A: 159: Tyr A: 63: Glu A: 7: Tyr (Aromatic, non-charged polarity) A: 171: Tyr (Aromatic, non-charged polarity) A: 5: Met A: 59: Tyr	A: 159: Tyr A: 166: Asp (Polarity with negative charge) A: 63: Glu A: 59: Tyr A: 167: Gly (Aliphatic, polarity without charge) A: 163: Thr (Hydroxyl, polarity without charge) A: 170: Arg (Polarity with positive charge)
4	S3H	CYHLYGTTL	A: 156: Gln A: 159: Tyr A: 99: Phe	A: 156: Gln A: 159: Tyr A: 99: Phe
5	L9F	CYSLYGTTF	A: 143: Thr A: 146: Lys A: 84: Tyr A: 77: Asn A: 80: Ile A: 147: Trp (Aromatic, non-polar) A: 123: Tyr	A: 84: Tyr A: 77: Asn A: 143: Thr A: 146: Lys A: 123: Tyr A: 80: Ile A: 95: Leu (Aliphatic, non-polar) A: 116: Tyr (Aromatic, non-charged polarity) A: 124: Ile (Aliphatic, non-polar)
6	Y2W	CWSLYGTTL	A: 70: Hie A: 63: Glu (Polarity with negative charge) A: 7: Tyr (Aromatic, non-charged polarity) A: 67: Val A: 99: Phe A: 45: Met (Sulfur, non-polar) A: 66: Lys A: 24: Ala (Aliphatic, non-polar)	A: 70: Hie A: 99: Phe A: 156: Gln (Amido, polarity without charge) A: 97: Met (Sulfur, non-polar) A: 66: Lys A: 159: Tyr (Aromatic, non-charged polarity) A: 67: Val
7	L9W	CYSLYGTTW	A: 143: Thr A: 146: Lys A: 84: Tyr (Aromatic, non-charged polarity) A: 77: Asn A: 80: Ile (Aliphatic, non-polar) A: 147: Trp A: 123: Tyr	A: 143: Thr A: 77: Asn A: 116: Tyr (Aromatic, non-charged polarity) A: 95: Leu (Aliphatic, non-polar) A: 146: Lys A: 117: Ala (Aliphatic, non-polar) A: 81: Ala (Aliphatic, non-polar) A: 118: Tyr (Aromatic, non-charged polarity) A: 147: Trp A: 123: Tyr
8	I4Y	HYNYVTFCC	none	A: 66: Lys (Polarity with positive charge)
9	V5Y	HYNIYTFCC	A: 156: Gln A: 155: Gln	A: 155: Gln A: 156: Gln

10	F7Y	HYNIVTYCC	A: 77: Asn A: 73: Thr A: 156: Gln (Amido, polarity without charge) A: 114: Hie (Polarity with positive charge) A: 147: Trp (Aromatic, non-polar) A: 133: Trp (Aromatic, non-polar)	A: 77: Asn A: 73: Thr A: 152: Val (Aliphatic, non-polar) A: 155: Gln (Amido, polarity without charge)
11	N3H	HYHIVTFCC	A: 156: Gln A: 159: Tyr A: 66: Lys A: 99: Phe	A: 156: Gln A: 159: Tyr A: 99: Phe A: 66: Lys
12	C9F	HYNIVTFCF	A: 146: Lys A: 77: Asn A: 147: Trp A: 80: Ile	A: 146: Lys A: 84: Tyr (Aromatic, non-charged polarity) A: 143: Thr (Hydroxyl, polarity without charge) A: 123: Tyr (Aromatic, non-charged polarity) A: 77: Asn A: 80: Ile A: 116: Tyr (Aromatic, non-charged polarity) A: 95: Leu (Aliphatic, non-polar) A: 147: Trp
13	Y2W	HWNIVTFCC	A: 70: Hie A: 63: Glu A: 66: Lys A: 7: Tyr A: 99: Phe (Aromatic, non-polar) A: 22: Phe (Aromatic, non-polar) A: 9: Ser (Hydroxyl, polarity without charge) A: 159: Tyr A: 67: Val	A: 63: Glu A: 70: Hie A: 67: Val A: 7: Tyr A: 24: Ala (Aliphatic, non-polar) A: 66: Lys A: 159: Tyr A: 25: Val (Aliphatic, non-polar) A: 45: Met (Sulfur, non-polar)
14	C9W	HYNIVTFCW	A: 146: Lys A:7 7: Asn A: 147: Trp A: 80: Ile	A: 143: Thr (Hydroxyl, polarity without charge) A: 77: Asn A: 146: Lys A: 95: Leu (Aliphatic, non-polar) A: 123: Tyr (Aromatic, non-charged polarity) A: 80: Ile A: 81: Ala (Aliphatic, non-polar) A: 117: Ala (Aliphatic, non-polar) A: 116: Tyr (Aromatic, non-charged polarity) A: 147: Trp A: 118: Tyr (Aromatic, non-charged polarity)

Table 4. The changes of the interaction formation between modified peptide and HLA

No.	Before Residue Replacement-Position-After Residue Replacement	Peptide Sequences	Before Residue Replacement					After Residue Replacement					Differences of Replacement				
			HB	Salt Bridges	Pi Stacking	Disulfides	vdW Clash	HB	Salt Bridges	Pi Stacking	Disulfides	vdW Clash	HB	Salt Bridges	Pi Stacking	Disulfides	vdW Clash
1	L4Y	CYSYYGTTL	0	0	0	0	0	0	0	0	0	0	0	0	0	0	0
2	T7Y	CYSLYGYTL	0	0	0	0	0	1	0	1	0	0	1	0	1	0	0
3	C1H	HYSLYGTTL	2	1	0	0	2	3	1	0	0	3	1	0	0	0	1
4	S3H	CYHLYGTTL	1	0	0	0	2	1	0	0	0	1	0	0	0	0	-1
5	L9F	CYSLYGTTF	4	1	0	0	1	4	1	1	0	2	0	0	1	0	1
6	Y2W	CWSLYGTTL	2	0	2	0	0	0	0	2	0	1	-2	0	0	0	1
7	L9W	CYSLYGTTW	4	1	0	0	1	2	1	1	0	3	-2	0	1	0	2
8	I4Y	HYNYVTFCC	0	0	0	0	0	0	0	0	0	0	0	0	0	0	0
9	V5Y	HYNIYTFCC	0	0	0	0	0	0	0	0	0	2	0	0	0	0	2
10	F7Y	HYNIVTYCC	1	0	0	0	0	1	0	0	0	0	0	0	0	0	0
11	N3H	HYHIVTFCC	1	0	0	0	0	1	0	0	0	0	0	0	0	0	0
12	C9F	HYNIVTFCF	1	1	0	0	1	3	1	1	0	5	2	0	1	0	4
13	Y2W	HWNIVTFCC	3	0	1	0	2	1	0	3	0	2	-2	0	2	0	0
14	C9W	HYNIVTFCW	1	1	0	0	1	3	1	2	0	0	2	0	2	0	-1

Table 5. Changes of complementary area of residue on the modified peptides to HLA

No.	Before Residue Replacement-Position-After Residue Replacement	Peptide Sequences	Surface Complementarity			Buried SASA		
			Before Residue Replacement	After Residue Replacement	Differences of Replacement	Before Residue Replacement	After Residue Replacement	Differences of Replacement
1	L4Y	CYSYYGTTL	0.67	0.87	0.2	0.553	0.423	-0.13
2	T7Y	CYSLYGYTL	0.89	0.74	-0.15	0.586	0.647	0.061
3	C1H	HYSLYGTTL	0.8	0.74	-0.06	0.848	0.863	0.015
4	S3H	CYHLYGTTL	0.84	0.66	-0.18	0.955	0.942	-0.013
5	L9F	CYSLYGTTF	0.8	0.83	0.03	0.981	0.977	-0.004
6	Y2W	CWSLYGTTL	0.79	0.83	0.04	0.976	0.976	0
7	L9W	CYSLYGTTW	0.8	0.77	-0.03	0.981	0.962	-0.019
8	I4Y	HYNYVTFCC	0.56	0.85	0.29	0.335	0.373	0.038
9	V5Y	HYNIYTFCC	0.7	0.36	-0.34	0.851	0.336	-0.515
10	F7Y	HYNIVTYCC	0.75	0.81	0.06	0.972	0.731	-0.241
11	N3H	HYHIVTFCC	0.87	0.86	-0.01	0.977	0.982	0.005
12	C9F	HYNIVTFCF	0.69	0.87	0.18	0.916	0.991	0.075
13	Y2W	HWNIVTFCC	0.77	0.82	0.05	0.992	0.996	0.004
14	C9W	HYNIVTFCW	0.69	0.87	0.18	0.916	0.975	0.059

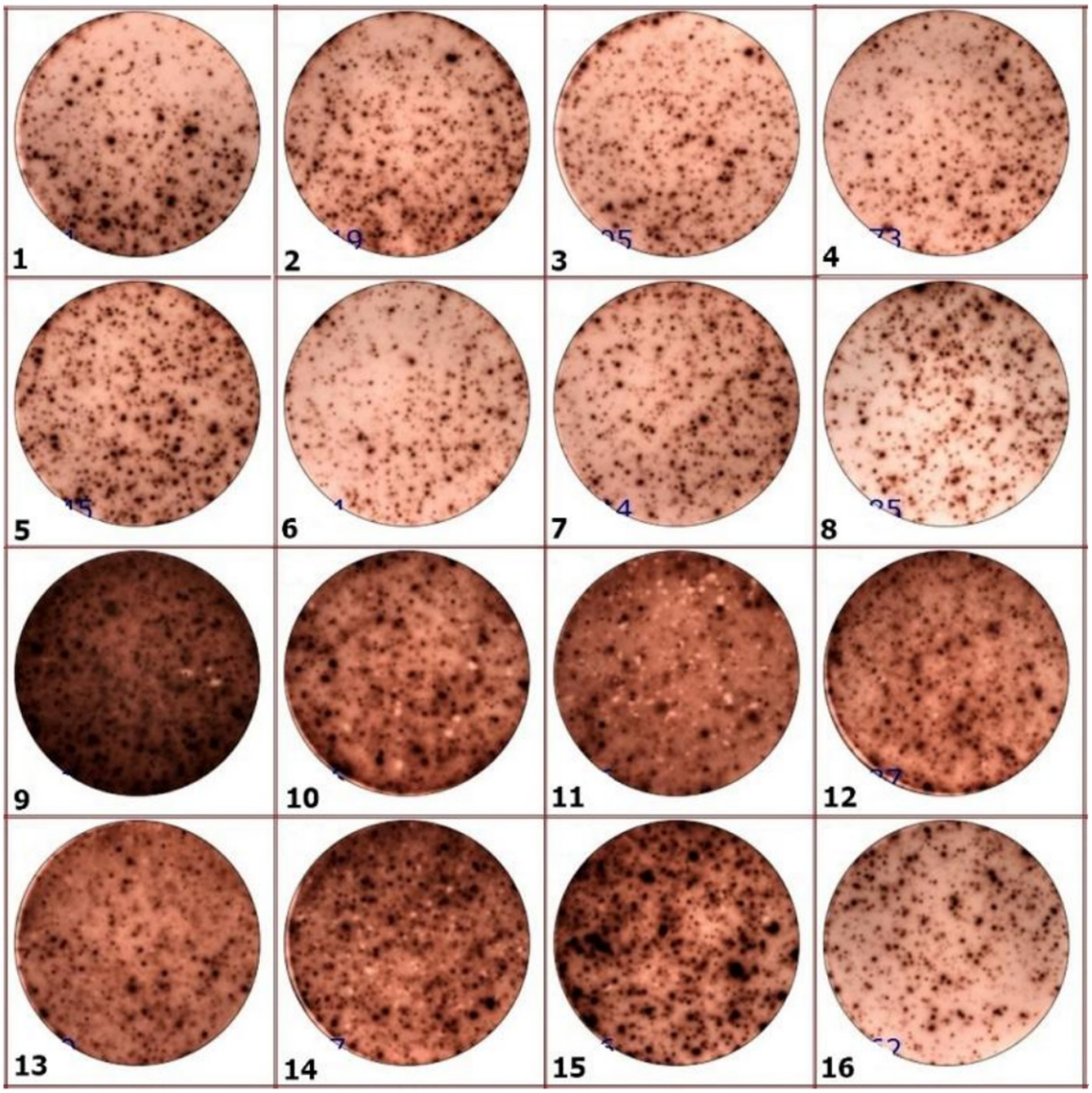

Figure 1. Activation of HLA-A*2402 allele CTL cells by Polypeptide DC vaccines before and after modification. Number 1 to 16 were represented for CYSLYGTTL, CYSYYGTTL, CYSLYGYTL, HYSLYGTTL, CYHLYGTTL, CYSLYGTTF, CWSLYGTTL, CYSLYGTTW, HYNIVTFCC, HYNYVTFCC, HYNIYTFCC, HYNIVTYCC, HYHIVTFCC, HYNIVTFCF, HWNIVTFCC and HYNIVTFCW, respectively. The round spots with dark center and blurred edges were regarded as the activated CTL cells.

types, predicted peptides with higher binding scores did not necessarily mean immunogenicity. However, peptide binding predictors remained useful and could reduce many candidate epitopes that must be verified by experiments [10]. Antigen processing and presentation was a complex multi-step process. Computer epitope prediction may be a useful tool, but it may require comprehensive experiments and verification in each patient to screen tumor antigens reliably [3]. The ability to correlate computer-aided design parameters, such as molecular dynamics simulation and molecular docking with *in vitro* competitive binding experiments and CTL cell activation tests, was critical for predicting antigen peptides with high HLA affinity. In this study, forming a hydrogen bond and a salt bridge reduced the number of CTL cells activated by p-HLA complex. We will further investigate whether inhibiting the interaction formation of hydrogen bonds and van der Waals forces between the polypeptide and HLA

Table 6. Spot values of the CTL cells with HLA-A*2402 allele activated by polypeptides DC vaccines before and after modification

No.	Before Residue Replacement-Position-After Residue	Peptide Sequences	Average	Standard Deviation	*P value* (Dunn's t test)
1	original	CYSLYGTTL	89.00	3.74	none
2	L4Y	CYSYYGTTL	112.33	10.14	0.351
3	T7Y	CYSLYGYTL	102.00	5.72	0.56
4	C1H	HYSLYGTTL	144.33	20.29	0.085
5	S3H	CYHLYGTTL	111.67	24.07	0.414
6	L9F	CYSLYGTTF	64.33	8.18	0.512
7	Y2W	CWSLYGTTL	100.67	11.95	0.63
8	L9W	CYSLYGTTW	184.33	17.15	0.031*
9	original	HYNIVTFCC	31.33	13.22	none
10	I4Y	HYNYVTFCC	49.00	4.97	0.782
11	V5Y	HYNIYTFCC	42.00	7.87	0.896
12	F7Y	HYNIVTYCC	118.67	13.12	0.006**
13	N3H	HYHIVTFCC	63.67	5.79	0.343
14	C9F	HYNIVTFCF	53.33	4.50	0.54
15	Y2W	HWNIVTFCC	102.67	17.00	0.033*
16	C9W	HYNIVTFCW	142.67	15.15	0.001**

*$P < 0.05$, **$P < 0.01$.

Table 7. The changes of molecular simulation parameters of peptides before and after modification to HLA

No.	Before Residue Replacement-Position-After Residue	Position	Peptide Sequences	Total number of HB	Total number of Salt Bridges	Total number of Pi-stacking	Total number of vdW Clash	Average values of Surface Complementarity	Average values of Buried SASA
1	original	-	CYSLYGTTL	10	2	4	7	0.71	0.72
2	L4Y	4	CYSYYGTTL	10	2	2	8	0.80	0.78
3	T7Y	7	CYSLYGYTL	8	1	3	6	0.76	0.69
4	C1H	1	HYSLYGTTL	9	2	2	6	0.71	0.68
5	S3H	3	CYHLYGTTL	8	2	4	5	0.76	0.72
6	L9F	9	CYSLYGTTF	9	2	3	10	0.77	0.73
7	Y2W	2	CWSLYGTTL	8	2	2	3	0.75	0.74
8	L9W	9	CYSLYGTTW	7	1	2	7	0.78	0.74
9	original	-	HYNIVTFCC	11	2	1	6	0.73	0.77
10	I4Y	4	HYNYVTFCC	11	2	3	7	0.77	0.76
11	V5Y	5	HYNIYTFCC	14	2	2	12	0.75	0.76
12	F7Y	7	HYNIVTYCC	12	2	1	7	0.78	0.74
13	N3H	3	HYHIVTFCC	10	2	3	6	0.75	0.73
14	C9F	9	HYNIVTFCF	11	2	6	8	0.79	0.77
15	Y2W	2	HWNIVTFCC	12	2	3	8	0.73	0.79
16	C9W	9	HYNIVTFCW	10	1	5	3	0.78	0.78

can weaken the number of CTL cells activated by the polypeptide, and then what will happen to the affinity, stability and total binding free energy between the two in this state?

In a related study [11], 837 peptides bound by MHC II alleles were simulated, and the results were compared with molecular dynamics simulations. The Rosetta backrub method optimized the conformation and generated a scoring matrix to predict the binding differences. According to the findings, the positive predictive rate of binding a single residue mutant peptide to MHC II was less than 60% based on the existing model. Concurrently, the scoring method of molecular dynamics could be increased

Table 8. The correlation among the spots number of CTL cells activation and molecular simulation parameters

Spots number of CTL cells activation		
Position	Correlation Coefficient	0.233
	P value	0.386
DELTA TOTAL	Correlation Coefficient	0.303
	P value	0.255
VDWAALS	Correlation Coefficient	-0.091
	P value	0.736
EEL	Correlation Coefficient	0.102
	P value	0.707
EGB	Correlation Coefficient	0.233
	P value	0.385
ESURF	Correlation Coefficient	-0.067
	P value	0.807
DELTA G gas	Correlation Coefficient	0.043
	P value	0.875
DELTA G solv	Correlation Coefficient	0.229
	P value	0.393
Total number of HB	Correlation Coefficient	-0.560*
	P value	0.024
Total number of Salt Bridges	Correlation Coefficient	-0.571*
	P value	0.021
Total number of Pi-stacking	Correlation Coefficient	-0.057
	P value	0.835
Total number of vdW Clash	Correlation Coefficient	-0.409
	P value	0.116
Average values of Surface Complementarity	Correlation Coefficient	0.154
	P value	0.57
Average values of Buried SASA	Correlation Coefficient	-0.239
	P value	0.372

*$P < 0.05$.

to 86%. A structural basis was provided for developing a simple score matrix to better predict the binding of single-point mutant peptides to MHC II molecules and to distinguish binding peptides from non-binding peptides at a reasonable level using molecular simulation. In addition, a study [12] on the conformational changes in and around MHC binding slot caused by neo-antigen epitopes suggested that structural parameters, including solvent-accessible surface area (SASA) of the new epitope, and the position and spatial configuration of mutant residues in the sequence, could be used to improve the prediction efficacy of new immunogenic epitopes. Another study found that combining the widely used sequence-based artificial neural network method NetMHCpan 4.0 with three-dimensional structure modeling significantly improved statistical specificity and reduced the number of false positives. In addition, the structure-based predictor was used to screen candidates generated using NetMHCpan 4.0, and positive predictive values of peptides correctly predicted as strong binding (i.e., Kd < 100 nM) were increased from 40% to 52% ($P = 0.027$) [13]. Recently, it has been found [14] that hydrogen bonds or pi interactions in MHC-restricted antigen peptides lead to an α-right helix or β-rotation conformations of the peptide, which could induce different immune responses or not. The structure and function of synthetic peptides could be regulated by specific amino acid substitution, and intermolecular interactions (hydrogen

bonds or pi-interactions) could be formed by immune protection to induce protein structure (IMPIPS). Peripheral flanking residues stabilize MHC-II-IMPIPS-TCR interactions and develop lasting protective immune memory [15]. Non-covalent interactions allowed HLA to bind to peptides. Peptide binding grooves (PBG) were made up of pockets A through F, and each had a preference for different biochemical properties such as charge, size, hydrophobicity, polarity and peptide composition [16]. The critical sites for HLA-I binding were at P2 or P3 and C-terminal (F pocket, hydrophobic or charged), known as anchored residues. The substituting residues on the anchoring residues would significantly change the binding stability of peptide-HLA complex [17]. Neo-antigens were classified into three categories: first, the mutation (single residue substitution) occurred on the unanchored residue of the existing "self" peptide; second, the mutation occurred on the anchored residue; third, the mutation did not occur on the peptide presented by the host HLA [18]. Many TCRs that recognized the new antigens of group 1 could be eliminated due to their high similarity to wild-type "self" peptides [19, 20]. The mutation peptides of the second group were transformed from a previous non-HLA binding sequence into a new non-self epitope. Therefore, for the first group, the predicted binding affinity was similar. In contrast, for the second group, the binding affinity of the mutant peptides would be much higher than the wild-type sequences [6], and formed a specific interaction with homologous TCR and produced a strong T cell response [21, 22]. In addition, it was associated with a better prognosis [23, 24]. In this study, single residue replacement on the antigens promoted the formation of pi-stacking interactions between peptides and HLA-A*2402. The total free energy values, the number of intermolecular interactions and the level of activated CTL cells were mainly increased, particularly in 9^{th} residue substitutions like C9F and C9W. Do the above rules apply to the other common alleles of HLA-I molecules and their restricted antigenic polypeptides? Whether the residues of the other positions on the polypeptides that fail to form pi-stacking interaction with HLA molecules can promote the formation of pi-stacking interaction through residue substitution. Will the activation of the specific CTL cells by the single residue replaced polypeptide have an effect of amplifying or weakening the response? We will continue follow-up research to clarify the law.

This study aimed to identify the characteristics of antigens with high immunogenicity by investigating the interaction between peptide and HLA-A*2402 and then to improve their immunogenicity through single residue substitution based on those characteristics. In the future, we will investigate the factors that influence the immunity and specificity of the new antigen with HLA and TCR, as well as the related parameters that enhance the immunogenicity of the new antigen and HLA without compromising its TCR specificity, to transform the new tumor antigen with high immunogenicity.

Acknowledgements

Supported by the grant from Major Project of Hangzhou Science and Technology Plan (No. 202004A21), the Youth Project of Natural Science Foundation of China (No. 82004129), the General Project of Natural Science Foundation of Zhejiang Province (No. LY22H290002), and the Research Project of Zhejiang Chinese Medical University (No. 2021JKZKTS051B).

Disclosure of conflict of interest

None.

Address correspondence to: Ling-Zhi Chen, Department of Blood Transfusion, The First Hospital of Jiaxing, Affiliated Hospital of Jiaxing University, No. 1882 Central South Road, Nanhu District, Jiaxing 314001, Zhejiang, China. E-mail: 27320-28753@qq.com

References

[1] Lee MY, Jeon JW, Sievers C and Allen CT. Antigen processing and presentation in cancer immunotherapy. J Immunother Cancer 2020; 8: e001111.

[2] Hoffmann MM and Slansky JE. T-cell receptor affinity in the age of cancer immunotherapy. Mol Carcinog 2020; 59: 862-870.

[3] Crean RM, MacLachlan BJ, Madura F, Whalley T, Rizkallah PJ, Holland CJ, McMurran C, Harper S, Godkin A, Sewell AK, Pudney CR, van der Kamp MW and Cole DK. Molecular rules underpinning enhanced affinity binding of human T cell receptors engineered for immunotherapy. Mol Ther Oncolytics 2020; 18: 443-456.

[4] Huang C, Chen J, Ding F, Yang L, Zhang S, Wang X, Shi Y and Zhu Y. Related parameters of affinity and stability prediction of HLA-A*2402 restricted antigen peptides based on molecular docking. Ann Transl Med 2021; 9: 673.
[5] Bonsack M, Hoppe S, Winter J, Tichy D, Zeller C, Küpper MD, Schitter EC, Blatnik R and Riemer AB. Performance evaluation of MHC class-I binding prediction tools based on an experimentally validated MHC-peptide binding data set. Cancer Immunol Res 2019; 7: 719-736.
[6] Jurtz V, Paul S, Andreatta M, Marcatili P, Peters B and Nielsen M. NetMHCpan-4.0: improved peptide-MHC class I interaction predictions integrating eluted ligand and peptide binding affinity data. J Immunol 2017; 199: 3360-3368.
[7] O'Donnell TJ, Rubinsteyn A and Laserson U. MHCflurry 2.0: improved pan-allele prediction of MHC class I-presented peptides by incorporating antigen processing. Cell Syst 2020; 11: 42-48, e7.
[8] Tang Y, Wang Y, Wang J, Li M, Peng L, Wei G, Zhang Y, Li J and Gao Z. TruNeo: an integrated pipeline improves personalized true tumor neoantigen identification. BMC Bioinformatics 2020; 21: 532.
[9] Boehm KM, Bhinder B, Raja VJ, Dephoure N and Elemento O. Predicting peptide presentation by major histocompatibility complex class I: an improved machine learning approach to the immunopeptidome. BMC Bioinformatics 2019; 20: 7.
[10] Mei S, Li F, Leier A, Marquez-Lago TT, Giam K, Croft NP, Akutsu T, Smith AI, Li J, Rossjohn J, Purcell AW and Song J. A comprehensive review and performance evaluation of bioinformatics tools for HLA class I peptide-binding prediction. Brief Bioinform 2020; 21: 1119-1135.
[11] Ochoa R, Laskowski RA, Thornton JM and Cossio P. Impact of structural observables from simulations to predict the effect of single-point mutations in MHC class II peptide binders. Front Mol Biosci 2021; 8: 636562.
[12] Zaidi N, Soban M, Chen F, Kinkead H, Mathew J, Yarchoan M, Armstrong TD, Haider S and Jaffee EM. Role of in silico structural modeling in predicting immunogenic neoepitopes for cancer vaccine development. JCI Insight 2020; 5: e136991.
[13] Aranha MP, Jewel YSM, Beckman RA, Weiner LM, Mitchell JC, Parks JM and Smith JC. Combining three-dimensional modeling with artificial intelligence to increase specificity and precision in peptide-MHC binding predictions. J Immunol 2020; 205: 1962-1977.
[14] Reyes C, Moreno-Vranich A and Patarroyo ME. The role of pi-interactions and hydrogen bonds in fully protective synthetic malaria vaccine development. Biochem Biophys Res Commun 2017; 484: 501-507.
[15] Curtidor H, Reyes C, Bermúdez A, Vanegas M, Varela Y and Patarroyo ME. Conserved binding regions provide the clue for peptide-based vaccine development: a chemical perspective. Molecules 2017; 22: 2199.
[16] Madden DR. The three-dimensional structure of peptide-MHC complexes. Annu Rev Immunol 1995; 13: 587-622.
[17] Istrail S, Florea L, Halldórsson BV, Kohlbacher O, Schwartz RS, Yap VB, Yewdell JW and Hoffman SL. Comparative immunopeptidomics of humans and their pathogens. Proc Natl Acad Sci U S A 2004; 101: 13268-13272.
[18] Fritsch EF, Rajasagi M, Ott PA, Brusic V, Hacohen N and Wu CJ. HLA-binding properties of tumor neoepitopes in humans. Cancer Immunol Res 2014; 2: 522-529.
[19] Germain RN. T-cell development and the CD4-CD8 lineage decision. Nat Rev Immunol 2002; 2: 309-322.
[20] Spits H. Development of alphabeta T cells in the human thymus. Nat Rev Immunol 2002; 2: 760-772.
[21] Sim MJW, Lu J, Spencer M, Hopkins F, Tran E, Rosenberg SA, Long EO and Sun PD. High-affinity oligoclonal TCRs define effective adoptive T cell therapy targeting mutant KRAS-G12D. Proc Natl Acad Sci U S A 2020; 117: 12826-12835.
[22] Tran E, Robbins PF, Lu YC, Prickett TD, Gartner JJ, Jia L, Pasetto A, Zheng Z, Ray S, Groh EM, Kriley IR and Rosenberg SA. T-cell transfer therapy targeting mutant KRAS in cancer. N Engl J Med 2016; 375: 2255-2262.
[23] Ghorani E, Rosenthal R, McGranahan N, Reading JL, Lynch M, Peggs KS, Swanton C and Quezada SA. Differential binding affinity of mutated peptides for MHC class I is a predictor of survival in advanced lung cancer and melanoma. Ann Oncol 2018; 29: 271-279.
[24] Rech AJ, Balli D, Mantero A, Ishwaran H, Nathanson KL, Stanger BZ and Vonderheide RH. Tumor immunity and survival as a function of alternative neopeptides in human cancer. Cancer Immunol Res 2018; 6: 276-287.